SRC TR 89-21

Tethered Satellite System Stability

by

D. C. Liaw

and

E. H. Abed

Tethered Satellite System Stability

D.-C. Liaw and E.H. Abed

Department of Electrical Engineering
and the Systems Research Center
University of Maryland
College Park, MD 20742 USA

Abstract

Issues of stability of the Tethered Satellite System (TSS) during station-keeping, deployment and retrieval are considered. The basic nonlinear equations of motion of the TSS are derived using the system Lagrangian. Using the Hopf bifurcation theorem, tension control laws are established which guarantee the stability of the system during the station-keeping mode. A constant angle control method is hypothesized for subsatellite deployment and retrieval. It is proved that this control law results in stable deployment but unstable retrieval. An enhanced control law for deployment is also proposed, which entails use of the constant angle method followed by a station-keeping control law once the tether length is sufficiently near the desired value. Simulations are given to illustrate the conclusions.

I. Introduction

The Tethered Satellite System (TSS) [1]-[8] consists of a satellite and subsatellite connected by a tether, in orbit around the Earth. Many potential applications of the TSS have been proposed, including deployment of scientific instruments and study of the Earth's magnetic field [1], [12]. Station-keeping, deployment and retrieval of payloads are the three major modes of operation.

Arnold [2] proposed a constant angle method for deployment and retrieval of subsatellite of the tethered satellite system. In [2], the satellite and subsatellite are modeled as point masses and the tether is assumed massless and of length small compared with the radius of the satellite's orbit. Based on these assumptions, Arnold obtained an approximate model of the TSS by applying the gravity-gradient method and argued that this constant angle scheme would result in stable deployment and unstable retrieval.

One goal of this paper is to give a proof of the validity of these conclusions. First, however, general dynamic equations for the TSS are derived by using the system Lagrangian. The applied tension control force is assumed to be the only external force acting on the TSS. Next we consider stabilization of the TSS during the station-keeping mode, in which the tether's length is regulated to remain nearly fixed. We observe from linear analysis at the system equilibria the presence of two pairs of pure imaginary eigenvalues in the absence of feedback. This suggests the possibility of librations superimposed upon the orbital motion. It is found that nonlinear stability analysis is needed to study stability and stabilization of the TSS during station-keeping. The program of [15], which considers Hopf bifurcation control algorithms, is employed to derive stabilizing control laws. Both linear and nonlinear feedback controls are achieved which guarantee asymptotic stability.

Viewing the tether length as an input variable for deployment and retrieval of the TSS, a constant in-plane angle control scheme is considered next. Within this setting, we prove stability of constant-angle deployment and instability of constant-angle retrieval. This is achieved through the construction of appropriate Liapunov-like functions and by appealing to the finite-time stability theory. A new control strategy for deployment of the subsatellite is also proposed. This control law consists of the constant angle scheme followed by the stabilizing station-keeping control.

Finally, simulation results are given to demonstrate the analytical conclusions of the paper.

Notation

E - Earth

S - Satellite

m - Subsatellite and its mass

G - Gravitational constant

M, m_s - Mass of the Earth, mass of the satellite

(x_m, y_m, z_m) - Earth-based rotating Cartesian coordinates of subsatellite, with z_m in the local outgoing vertical direction, and x_m in the direction of motion of the satellite in its orbit (see Figure 1)

$(\hat{x}_m, \hat{y}_m, \hat{z}_m)$ - Inertial coordinates of subsatellite

$(\hat{x}_s, \hat{y}_s, \hat{z}_s)$ - Inertial coordinates of the satellite

Ω - Constant angular velocity of the satellite in circular orbit

θ, ϕ - In-plane angle and out-of-plane angle of subsatellite relative to local vertical

$\omega_\phi := \dot{\phi}$, $\omega_\theta := \dot{\theta}$, ℓ - Tether length, $v := \dot{\ell}$

r_0, r_m - Radius of the satellite orbit, radius of subsatellite orbit

$(\cdot)^*$ - Evaluation at equilibrium

τ_θ, τ_ϕ - Torques in directions θ, ϕ

F_ℓ - Force along tether (i.e., the applied tension force)

$\mathbf{F} := \frac{\tau_\theta}{\ell \cos\phi}\hat{\theta} + \frac{\tau_\phi}{\ell}\hat{\phi} + F_\ell \hat{\ell}$, where a hat indicates a unit vector in the given direction

II. System Dynamic Equations

The coordinate system of a typical tethered satellite system is depicted in Figure 1. Referring to this coordinate system, we make the following *simplifying assumptions*: The satellite and the subsatellite are point masses. Their masses are related as $m_s \gg m$, and hence the center of mass of the TSS may be taken to coincide with the satellite. The tether is massless and rigid, and the gravitational attraction between the subsatellite and the satellite is neglected. Finally, the TSS experiences no aerodynamic drag forces, and the satellite is in a circular orbit around the Earth.

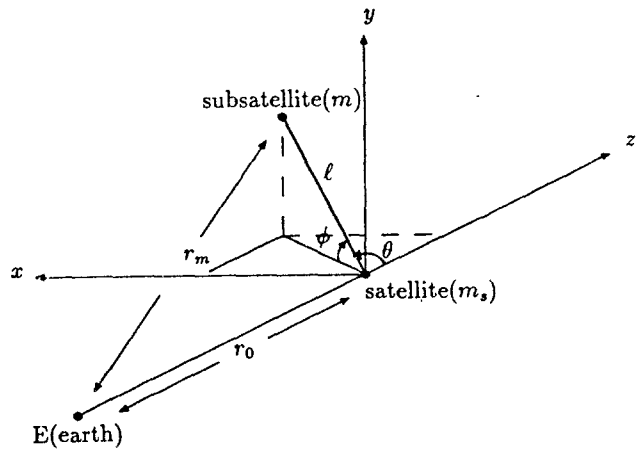

Figure 1. Coordinate System of the TSS

It is obvious from Figure 1 that we have following relationships (see the notation list in Section I).

$$x_m = \ell \cos\phi \sin\theta \tag{1}$$

$$y_m = \ell \sin\phi \tag{2}$$

$$z_m = r_0 + \ell \cos\phi \cos\theta \tag{3}$$

$$r_m^2 = r_0^2 + \ell^2 + 2r_0\ell \cos\phi \cos\theta \tag{4}$$

The inertial coordinates of the subsatellite and the satellite are given as

$$\begin{pmatrix} \hat{x}_m \\ \hat{y}_m \\ \hat{z}_m \end{pmatrix} = \begin{pmatrix} \cos\Omega t & 0 & \sin\Omega t \\ 0 & 1 & 0 \\ -\sin\Omega t & 0 & \cos\Omega t \end{pmatrix} \begin{pmatrix} x_m \\ y_m \\ z_m \end{pmatrix}, \tag{5a}$$

$$\begin{pmatrix} \hat{x}_s \\ \hat{y}_s \\ \hat{z}_s \end{pmatrix} = \begin{pmatrix} \cos\Omega t & 0 & \sin\Omega t \\ 0 & 1 & 0 \\ -\sin\Omega t & 0 & \cos\Omega t \end{pmatrix} \begin{pmatrix} 0 \\ 0 \\ r_0 \end{pmatrix}, \tag{5b}$$

where an implicit choice of time reference is understood.

The kinetic energy of the TSS is

$$KE = \frac{1}{2}m_s(\dot{\hat{x}}_s^2 + \dot{\hat{y}}_s^2 + \dot{\hat{z}}_s^2) + \frac{1}{2}m(\dot{\hat{x}}_m^2 + \dot{\hat{y}}_m^2 + \dot{\hat{z}}_m^2). \tag{6}$$

Using Eq. (5), this may be rewritten as

$$KE = \frac{1}{2}m_s\Omega^2 r_0^2 + \frac{1}{2}m\{\dot{\ell}^2 + \ell^2\dot{\phi}^2 + \ell^2\cos^2\phi(\dot{\theta}+\Omega)^2 + \Omega^2 r_0^2$$
$$+ 2\Omega r_0\dot{\ell}\cos\phi\sin\theta - 2\Omega r_0\ell\sin\phi\sin\theta\dot{\phi} + 2\Omega r_0\ell\cos\phi\cos\theta(\dot{\theta}+\Omega)\}. \tag{7}$$

The potential energy of the TSS is due to gravity and is given by

$$PE = -\frac{GMm_s}{r_0} - \frac{GMm}{r_m}. \tag{8}$$

The satellite is in a circular orbit, implying that it is in a zero-g orbit. Hence

$$\frac{GMm_s}{r_0^2} = m_s\Omega^2 r_0, \tag{9}$$

i.e., we can take $GM = \Omega^2 r_0^3$.

By writing the system Lagrangian $L = KE - PE$ and invoking the Lagrangian formulation of the system's dynamics, the equations of motion of the TSS are obtained as

$$\tau_\theta = m\ell^2 \cos^2\phi\{\ddot{\theta} + 2\frac{\dot{\ell}}{\ell}(\dot{\theta}+\Omega) - 2\tan\phi(\dot{\theta}+\Omega)\dot{\phi} + \frac{\Omega^2 r_0 \sin\theta}{\ell\cos\phi}(1-\frac{r_0^3}{r_m^3})\} \tag{10}$$

$$\tau_\phi = m\ell^2\{\ddot{\phi} + 2\frac{\dot{\ell}}{\ell}\dot{\phi} + \cos\phi\sin\phi(\dot{\theta}+\Omega)^2 + \frac{\Omega^2 r_0}{\ell}\cos\theta\sin\phi(1-\frac{r_0^3}{r_m^3})\} \tag{11}$$

$$F_\ell = m\{\ddot{\ell} - \ell(\dot{\phi})^2 - \ell\cos^2\phi(\dot{\theta}+\Omega)^2 + \frac{\Omega^2 r_0^3 \ell}{r_m^3} - \Omega^2 r_0\cos\phi\cos\theta(1-\frac{r_0^3}{r_m^3})\} \tag{12}$$

For the case $r_0 \gg \ell$, we have $r_m \simeq r_0$. Moreover, in this case Eq. (4) implies

$$1 - \frac{r_0^3}{r_m^3} \simeq 3\cos\phi\cos\theta\frac{\ell}{r_0}. \tag{13}$$

Hence, the approximate equation of motion for the system for the case $r_0 \gg \ell$ is obtained as

$$\begin{aligned}\mathbf{F} = {} & m\hat{\ell}\{\ddot{\ell} - \ell\dot{\phi}^2 - \ell\cos^2\phi(\dot{\theta}+\Omega)^2 + \ell\Omega^2 - 3\Omega^2\ell\cos^2\phi\cos^2\theta\} \\ & + m\hat{\theta}\{\ddot{\theta}\ell\cos\phi + 2(\dot{\theta}+\Omega)(\dot{\ell}\cos\phi - \ell\dot{\phi}\sin\phi) + 3\ell\Omega^2\cos\theta\cos\phi\sin\theta\} \\ & + m\hat{\phi}\{\ell\ddot{\phi} + 2\dot{\ell}\dot{\phi} + \ell\cos\phi\sin\phi(\dot{\theta}+\Omega)^2 + 3\ell\Omega^2\cos^2\theta\cos\phi\sin\phi\}.\end{aligned}$$

This agrees with a result of Arnold [2]. Note, however, that we do *not* require $r_0 \gg \ell$ below.

III. Stabilization of System During Station-Keeping Mode

To facilitate design of stabilizing control laws for the TSS, we first rewrite the system of second order equations (10)-(12) in state space form. This is possible under the assumption $\cos\phi \neq 0$ (i.e., $\phi \neq \pm\frac{\pi}{2}$). In addition, we assume that the only external force acting on the

TSS is the applied tension F_ℓ. Setting $\tau_\theta = \tau_\phi = 0$ in (10)-(12) and denoting $T := F_\ell$, the equations of motion in state space form are found to be

$$\dot{\phi} = \omega_\phi \tag{14}$$

$$\dot{\omega}_\phi = -\frac{2v}{\ell}\omega_\phi - \frac{1}{2}\sin(2\phi)(\omega_\theta + \Omega)^2 - \frac{\Omega^2 r_0}{\ell}\cos\theta\sin\phi(1 - \frac{r_0^3}{r_m^3}) \tag{15}$$

$$\dot{\theta} = \omega_\theta \tag{16}$$

$$\dot{\omega}_\theta = -\frac{2v}{\ell}(\omega_\theta + \Omega) + 2\tan\phi(\omega_\theta + \Omega)\omega_\phi - \frac{\Omega^2 r_0 \sin\theta}{\ell\cos\phi}(1 - \frac{r_0^3}{r_m^3}) \tag{17}$$

$$\dot{\ell} = v \tag{18}$$

$$\dot{v} = \ell\omega_\phi^2 + \ell\cos^2\phi(\omega_\theta + \Omega)^2 - \frac{\Omega^2 r_0^3 \ell}{r_m^3} + \Omega^2 r_0\cos\theta\cos\phi(1 - \frac{r_0^3}{r_m^3}) + \frac{T}{m} \tag{19}$$

With the tether length held constant ($\ell = \ell^*$), this system has precisely two equilibrium points (0,0,0,0,ℓ^*,0) and (0,0,π,0,ℓ^*,0). Moreover, the linearized system of Eqs. (14)-(17) at such an equilibrium is found to have two pairs of pure imaginary eigenvalues, given by

$$\lambda_{1,2} = \pm i\Omega\sqrt{1 + \frac{r_0}{\ell^*}(1 - \frac{r_0^3}{r_{m,0}^3})}, \tag{20}$$

$$\lambda_{3,4} = \pm i\Omega\sqrt{\frac{r_0}{\ell^*}(1 - \frac{r_0^3}{r_{m,0}^3})}, \tag{21}$$

where $r_{m,0} = r_0 + \ell^*$ at $\theta = 0$ and $r_{m,0} = r_0 - \ell^*$ at $\theta = \pi$. The pairs $\lambda_{1,2}$ and $\lambda_{3,4}$ of eigenvalues are associated with the out-of-plane and in-plane dynamics, respectively, suggesting that the TSS may undergo librations with two different frequencies superimposed upon the orbital motion, near either of the equilibria. In addition [9], the set $\phi = 0, \omega_\phi = 0$ is an invariant manifold for Eqs. (14)-(19), regardless of the tension control force T. Although this implies the uncontrollability of the system, a tension control law still can be designed to guarantee asymptotic stability.

Stabilizability will first be studied at the equilibrium point $x_0 = (0,0,0,0,\ell^*,0)^T$. Apply a linear tension control law $T = -m(U + k_1\theta + k_2\omega_\theta + k_3\tilde{\ell} + k_4 v)$, where $k_i, i = 1,\cdots,6$

are constant control gains, $\tilde{\ell} := \ell - \ell^*$ and

$$U := \frac{(3r_0^2\ell^* + 3r_0\ell^{*2} + \ell^{*3})\Omega^2}{(r_0 + \ell^*)^2}. \tag{22}$$

The characteristic equation of the linearized closed-loop model of system (14)-(19) is found, after some manipulation, to be

$$(\lambda^2 + a_1^2)\,(\lambda^4 + k_4\lambda^3 + b_1\lambda^2 + b_2\lambda + b_3) = 0, \tag{23}$$

where

$$a_1 = (\frac{4r_0^3 + 6r_0^2\ell^* + 4r_0\ell^{*2} + \ell^{*3}}{(r_0 + \ell^*)^3})^{0.5}\Omega, \tag{24}$$

$$b_1 = k_3 - \frac{(2r_0\ell^{*2} + \ell^{*3})\Omega^2}{(r_0 + \ell^*)^3} - \frac{2\Omega k_2}{\ell^*} + 4\Omega^2, \tag{25}$$

$$b_2 = \frac{k_4(3r_0^3 + 3r_0^2\ell^* + r_0\ell^{*2})\Omega^2}{(r_0 + \ell^*)^3} - \frac{2\Omega k_1}{\ell^*}, \tag{26}$$

$$b_3 = \frac{(3r_0^3 + 3r_0^2\ell^* + r_0\ell^{*2})\Omega^2}{(r_0 + \ell^*)^3}(k_3 - \frac{(3r_0^3 + 3r_0^2\ell^* + 3r_0\ell^{*2} + \ell^{*3})\Omega^2}{(r_0 + \ell^*)^3}). \tag{27}$$

By applying the Routh-Hurwitz test to Eq. (23), we obtain the following preliminary result.

Lemma 1. If the tension control force is given as $T = m(-U - k_1\theta - k_2\omega_\theta - k_3\tilde{\ell} - k_4 v)$, then the linearized closed-loop system of Eqs. (14)-(19) at the equilibrium point x_0 has a pair of pure imaginary eigenvalues and four eigenvalues with negative real parts, provided that the gains $k_i, i = 1, \ldots, 4$ satisfy the following two conditions:

(i) $b_1, b_2, b_3, k_4 > 0$

(ii) $k_4 b_1 b_2 - b_2^2 - k_4^2 b_3 > 0$

Here, the $b_i, i = 1, 2, 3$ are as given in (25)-(27).

Note that, by Eq. (23), the system (14)-(19) has an uncontrollable pair of pure imaginary eigenvalues $\pm i a_1$, unaffected by linear state feedback. It is easily checked that this holds even with feedback of states ϕ and ω_ϕ. The stability of the closed-loop system cannot, therefore, be determined from the linearized model. That is, this is an example of

a critical case in nonlinear stability. Stability results for Hopf bifurcation of one-parameter families of nonlinear systems can be employed in studying the stability of critical systems with a single pair of pure imaginary eigenvalues. For a discussion, see [15]. Two types of stabilizing tension control laws are given in the next two theorems for the station-keeping application. Theorem 1 involves the use of linear state feedbacks and Theorem 2 accounts for a class of nonlinear feedbacks. Details, proofs and simpler results in the form of corollaries can be found in [13].

Theorem 1. If a linear state feedback controller T of the type specified in Lemma 1 is applied, with

$$(\frac{a_4}{2} + \frac{\ell^* a_1^2}{2} - \frac{\ell^*}{4}(k_3 - a_3))d_1 - \frac{1}{2}k_4 a_1 \ell^* d_2 < 0,$$

then the equilibrium point x_0 is rendered asymptotically stable for the system (14)-(19), where a_1 is as given in (24), and where

$$d_1 = k_1 + \frac{\ell^* k_4}{2\Omega}(a_2 + 4a_1^2), \tag{28}$$

$$d_2 = 2a_1(k_2 - 2\ell^*\Omega) + \frac{\ell^*(a_2 + 4a_1^2)}{4a_1\Omega}(a_3 + 4a_1^2 - k_3), \tag{29}$$

$$a_2 = -\frac{(3r_0^3 + 3r_0^2\ell^* + r_0\ell^{*2})\Omega^2}{(r_0 + \ell^*)^3}, \tag{30}$$

$$a_3 = \frac{(3r_0^3 + 3r_0^2\ell^* + 3r_0\ell^{*2} + \ell^{*3})\Omega^2}{(r_0 + \ell^*)^3}, \tag{31}$$

$$a_4 = -\frac{(8r_0^4\ell^* + 14r_0^3\ell^{*2} + 16r_0^2\ell^{*3} + 9r_0\ell^{*4} + 2\ell^{*5})\Omega^2}{2(r_0 + \ell^*)^4}. \tag{32}$$

Theorem 2. If the applied tension control force is given as $T = m(-U - k_1\theta - k_2\omega_\theta - k_3\tilde{\ell} - k_4 v - q_1\phi^2 - q_2\phi\omega_\phi - q_3\omega_\phi^2)$ with k_i, $i = 1, \ldots, 4$ satisfying the conditions of Lemma 1, then the system (14)-(19) is rendered asymptotically stable if the condition

$$(\frac{-q_1 + a_5}{2} + (\frac{\ell^* + q_3}{2})a_1^2 - (k_3 - a_3)\frac{\ell^*}{4})d_1 + \frac{a_1}{2}(-q_2 - \ell^* k_4)d_2 < 0$$

holds. Here, d_1, d_2 and $a_i, i = 1, \ldots, 4$ are as defined above.

Similar results can also be obtained for stabilizing the system at the equilibrium point $(0, 0, \pi, 0, \ell^*, 0)$ [16]. The details are omitted.

IV. Constant In-Plane Angle Control

In this section, we consider deployment and retrieval of the subsatellite in the tethered satellite system. Viewing ℓ as an external control input, the state equations (10)-(12) of the system are

$$\dot{\theta} = \omega_\theta \tag{33}$$

$$\dot{\omega}_\theta = -\frac{2\dot{\ell}}{\ell}(\omega_\theta + \Omega) + 2\tan\phi(\omega_\theta + \Omega)\omega_\phi - \frac{\Omega^2 r_0 \sin\theta}{\ell\cos\phi}(1 - \frac{r_0^3}{r_m^3}) \tag{34}$$

$$\dot{\phi} = \omega_\phi \tag{35}$$

$$\dot{\omega}_\phi = -\frac{2\dot{\ell}}{\ell}\omega_\phi - \frac{1}{2}\sin(2\phi)(\omega_\theta + \Omega)^2 - \frac{\Omega^2 r_0}{\ell}\cos\theta\sin\phi(1 - \frac{r_0^3}{r_m^3}). \tag{36}$$

At an equilibrium point $(\theta^*, \omega_\theta^*, \phi^*, \omega_\phi^*)$ of (33)-(36), if one exists, we have $\omega_\theta^* = \omega_\phi^* = 0$, and $\dot{\ell}$ is given (from Eq. (34)) by

$$\dot{\ell} = -\frac{\Omega r_0}{2\cos\phi^*}\sin\theta^*(1 - \frac{r_0^3}{(r_m^*(\ell))^3}) \tag{37}$$

and ϕ^* must satisfy either

$$\sin\phi^* = 0, \quad \text{or} \tag{38a}$$

$$\cos\phi^* = -\frac{r_0}{\ell}(1 - \frac{r_0^3}{(r_m^*(\ell))^3})\cos\theta^*, \tag{38b}$$

where

$$r_m^*(\ell) := (r_0^2 + \ell^2 + 2r_0\ell\cos\theta^*\cos\phi^*)^{1/2}. \tag{39}$$

Remark 1. In fact, only the case $\sin\phi^* = 0$ is realistic. To see this, consider momentarily the possibility (38*b*), which, using (33), would imply that at equilibrium $\dot{\ell}$ obeys

$$\dot{\ell} = \frac{\Omega\ell}{2}\tan\theta^*. \tag{40}$$

Since $-\frac{\pi}{2} \leq \phi^* \leq \frac{\pi}{2}$, we have $\cos\phi^* \geq 0$ (see Figure 1). Considering the possibilities $0 < \phi^* \leq \frac{\pi}{2}$ and $-\frac{\pi}{2} \leq \phi^* < 0$ separately, and referring to Figure 1 for the relative magnitudes of $r_m^*(\ell)$ and r_0, we find that the left and right sides of (38b) are then of opposite sign unless they both vanish. Hence, we obtain $\phi^* = \theta^* = \pm\frac{\pi}{2}$, implying $\dot{\ell}$ of (40) would be infinite.

□

In the light of Remark 1, we let $\phi^* = 0$. Eq. (37) now implies that at equilibrium ℓ satisfies

$$\dot{\ell} = -\frac{\Omega r_0}{2}(1 - \frac{r_0^3}{(\hat{r}_m^*(\ell))^3})\sin\theta^*, \tag{41}$$

where

$$\hat{r}_m^*(\ell) := (r_0^2 + \ell^2 + 2r_0\ell\cos\theta^*)^{1/2}. \tag{42}$$

This control law, which is referred to as the *constant in-plane angle control method*, results in the existence of an equilibrium point of (33)-(36). Moreover, the associated equilibrium point of system (33)-(36) will then be (θ^*, 0,0,0), where θ^* is the desired in-plane angle.

V. Stability Analysis of the TSS During Retrieval

Suppose for simplicity that $\dot{\ell} < 0$ throughout retrieval. From Eq. (41) we have

$$\dot{\ell} < 0 \iff -\frac{\Omega r_0}{2}(1 - \frac{r_0^3}{(\hat{r}_m^*(\ell))^3})\sin\theta^* < 0.$$

Denote by ℓ_i the initial (pre-retrieval) tether length. Then the condition for $\dot{\ell} < 0$ is that θ^* satisfies either $0 < \theta^* < \frac{\pi}{2}$ or $-\pi < \theta^* < \theta_1$ (see Figure 2), where $\theta_1 = \theta_1(\ell_i)$ is such that

$$\cos\theta_1 = -\frac{\ell_i}{2r_0}, \quad -\pi < \theta_1 < -\frac{\pi}{2}. \tag{43}$$

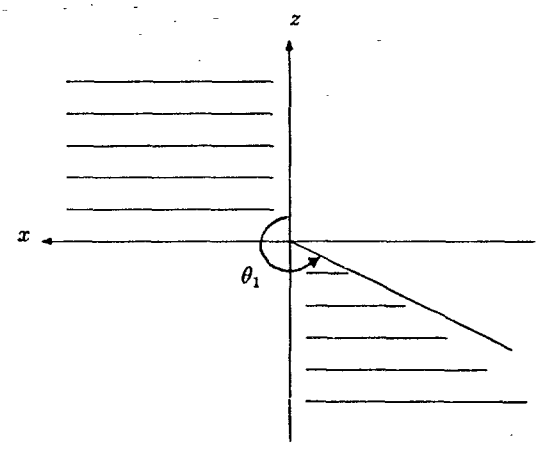

Figure 2. Retrieval Regions for θ^* with $\phi^* = 0$

From the discussion above, we have $\dot{\ell} < 0$ and $\ell > 0$ during retrieval by constraints. In addition, $\dot{\ell} = 0$ occurs only at $\ell = 0$. Hence, ℓ will approach 0 asymptotically.

Denoting $\tilde{\theta} := \theta - \theta^*$, the linearized system state equations at the equilibrium point $(\theta^*, 0, 0, 0)$ are found to be

$$\dot{\tilde{\theta}} = \omega_\theta \tag{44}$$

$$\dot{\omega}_\theta = (2\Omega\frac{\dot{\ell}}{\ell}\cot\theta^* + \frac{3\Omega^2 r_0^5}{(\hat{r}_m^*(\ell))^5}\sin^2\theta^*)\tilde{\theta} - 2\frac{\dot{\ell}}{\ell}\omega_\theta \tag{45}$$

$$\dot{\phi} = \omega_\phi \tag{46}$$

$$\dot{\omega}_\phi = (-\Omega^2 + 2\Omega\frac{\dot{\ell}}{\ell}\cot\theta^*)\phi - 2\frac{\dot{\ell}}{\ell}\omega_\phi \tag{47}$$

The *linearized* model of the system (33)-(36) is therefore seen to *decouple* into the subsystems (44)-(45) and (46)-(47). It follows from Lemma 2 and Theorem 3 below that these two decoupled subsystems are unstable for constant angle retrieval for any potential value of θ^* (see Figure 2), and that the original system (33)-(36) is then also unstable.

Lemma 2. If there is a constant $\delta > 0$ such that $b(t) > \delta$ for all $t \geq t_0$, then the origin is unstable for the system

$$\dot{x}_1 = x_2 \tag{48}$$

$$\dot{x}_2 = a(t)x_1 + b(t)x_2. \tag{49}$$

Proof: By the Abel-Jacobi-Liouville theorem (e.g., [10]), we have

$$\det(\Phi(t, t_0)) = \exp(\int_{t_0}^{t} b(s)ds),$$

where $\Phi(t, t_0)$ is the state transition matrix of the linear system (48)-(49). From the hypothesis, it now follows that $\det \Phi(t, t_0)$ approaches ∞ as $t \rightarrow \infty$. Hence, the origin is unstable.

□

Theorem 3. If $r_0 > \ell_i$, then the origin is unstable for the linearized system (44)-(47) during constant in-plane angle retrieval, and (θ^*,0,0,0) is an unstable equilibrium point of the original nonlinear system (33)-(36).

Proof: First, we show that there is a constant $\epsilon > 0$ such that $\frac{-\dot{\ell}}{\ell} > \epsilon$ for all $t \geq t_0$. By the discussion above, the tether length ℓ approaches 0 asymptotically. In addition, $\dot{\ell} = 0$ when $\ell = 0$. Applying L'Hôpital's Rule to (41)-(42), we obtain

$$\lim_{\ell \to 0} \frac{\dot{\ell}}{\ell} = \lim_{\ell \to 0} \frac{\partial \dot{\ell}}{\partial \ell} = -\frac{3}{2}\Omega \cos\theta^* \sin\theta^* \neq 0,$$

for any admissible θ^* (see Figure 2). Moreover, it is obvious that $-\frac{\dot{\ell}}{\ell} > 0$, for all $t \geq t_0$ during retrieval. Thus, $\frac{-\dot{\ell}}{\ell}$ is bounded and ϵ exists.

Next, we check the signs of the coefficients multiplying ω_θ and ω_ϕ in Eqs. (45) and (47), respectively. Since $0 < \epsilon < \frac{-\dot{\ell}}{\ell}$ for all $t \geq t_0$, Lemma 2 implies the origin is unstable for the two subsystems (44)-(45) and (46)-(47). This implies instability of the equilibrium point $(\theta^*, 0, 0, 0)$ of system (33)-(36) during constant in-plane angle retrieval.

□

VI. Stability Analysis of the TSS During Deployment

In this section, we consider application of the constant in-plane angle strategy of Section IV to subsatellite deployment. For simplicity, suppose that $\dot{\ell} > 0$ for all $t \geq t_0$. Since $\dot{\ell}$ is always positive in this consideration, one might expect that the tether length ℓ increases without bound. In reality, only a finite final tether length is meaningful for deployment. Stability of the TSS is hence only considered in a finite time interval, where Liapunov stability criteria cannot be employed. Results from finite-time stability shall be applied to study the behavior of this system.

Basic definitions and conditions for finite-time stability are given in Section VI.1. Then these finite-time stability criteria, especially the contractive stability criteria, are used to study the stability of the TSS during constant in-plane angle deployment. In addition to the proof of stability of deployment, a switching type control law combining constant angle deployment and station-keeping control is proposed to achieve asymptotic stability. Details of this are given in Section VI.2.

VI.1. Results on Finite-Time Stability

Consider a system given by

$$\dot{x} = f(t, x), \tag{50}$$

where $f: \Gamma \times R^n \to R^n$ and $\Gamma := [t_0, t_0 + T)$ for some $t_0 \in R$, $T > 0$. Let x_0 denote the initial condition of (50) at t_0, and let $\phi(t; t_0, x_0)$ be the solution of (50) at time t satisfying the initial condition. Then we have the following definitions [14].

Definition 1. System (50) is *finite-time stable* with respect to $(\alpha, \beta, \Gamma, ||\cdot||)$, $\alpha \leq \beta$, if for every trajectory $\phi(t; t_0, x_0)$ with $||x_0|| < \alpha$, we have $||\phi(t; t_0, x_0)|| < \beta$, $\forall\, t \in \Gamma$.

Definition 2. System (50) is *uniformly finite-time stable* with respect to $(\alpha, \beta, \Gamma, ||\cdot||)$, $\alpha \leq \beta$, if for any trajectory $\phi(t; s, x)$ with $||x|| < \alpha$, $\forall\, s \in \Gamma$, we have $||\phi(t; s, x)|| < \beta$, $\forall\, t \in \Gamma$.

Definition 3. System (50) is *quasi-contractively stable* with respect to $(\alpha, \gamma, \Gamma, ||\cdot||)$, $\gamma < \alpha$, if for any trajectory $\phi(t; t_0, x_0)$ with $||x_0|| < \alpha$, there exists $t_1 \in \Gamma$ so that $||\phi(t; t_0, x_0)|| < \gamma$, $\forall\, t \in [t_1, t_0 + T)$.

Definition 4. System (50) is *contractively stable* with respect to $(\alpha, \beta, \gamma, \Gamma, ||\cdot||)$, $\gamma < \alpha \leq \beta$, if it is finite-time stable with respect to $(\alpha, \beta, \Gamma, ||\cdot||)$ and quasi-contractively stable with respect to $(\alpha, \gamma, \Gamma, ||\cdot||)$.

For given α, β, Γ, and $||\cdot||$, a necessary and sufficient condition for uniform finite-time stability can be stated as follows.

Lemma 3 [14]. System (50) is uniformly finite-time stable with respect to $(\alpha, \beta, \Gamma, ||\cdot||)$, $\alpha < \beta$, if and only if there exists a continuous function $V(t, x)$ such that

$$\dot{V}(t, x) \leq 0, \quad \forall \ x \in \overline{B(\beta)}, \qquad t \in \Gamma, \tag{51}$$

$$V_M^{\delta}(t_1) < V_m^{\beta}(t_2), \quad \forall \ t_2 > t_1, \quad \forall \ \delta < \alpha, \quad t_1, t_2 \in \Gamma, \tag{52}$$

where

$$B(\beta) := \{x : ||x|| < \beta\}, \tag{53}$$

$||\cdot||$ denotes any norm on R^n, $\overline{B(\beta)}$ denotes the closure of $B(\beta)$, and

$$V_M^{\alpha}(t) := \sup_{||x||=\alpha} V(t, x), \tag{54}$$

$$V_m^{\alpha}(t) := \inf_{||x||=\alpha} V(t, x). \tag{55}$$

Here, $\dot{V}(t, x)$ is the time derivative of $V(t, x)$ along trajectories of system (50).

Stability properties of a system may be investigated without reference to the specific bounds on the states (i.e. α, β and γ). In the following lemma and theorem, two sufficient conditions are introduced for this type of stability. These provide a means for finding the associated bounds α, β, γ. Lemma 4 gives a sufficient condition for uniform finite-time stability. Theorem 4 then gives a relationship among T, α, β and γ providing a sufficient condition for contractive stability.

Lemma 4. System (50) is uniformly finite-time stable with respect to $(\alpha, \beta, \Gamma, ||\cdot||)$ for any given α and β with

$$0 < \alpha < \beta\sqrt{\frac{k_1}{k_2}} \leq \beta \leq r, \tag{56}$$

if there exist $r > 0$ and a continuously differentiable function $V(t,x)$ with

$$\dot{V}(t,x) \leq 0,$$
$$k_1||x||^2 \leq V(t,x) \leq k_2||x||^2, \tag{57}$$

for all $x \in \overline{B(r)}$, $t \in \Gamma$. Here, $0 < k_1 \leq k_2$ and the norm used is the Euclidean norm.

Proof: The result follows directly from condition (52) of Lemma 3.

□

In the next theorem, we introduce a condition on (50) and a relationship among T, α, β and γ guaranteeing finite-time *contractive* stability.

Theorem 4. System (50) is contractively stable with respect to $(\alpha, \beta, \gamma, \Gamma, ||\cdot||)$ for any triple α, β, γ with

$$\alpha\sqrt{\frac{k_2}{k_1} \cdot \exp(-\frac{k_3}{k_2}T)} \leq \gamma < \alpha < \sqrt{\frac{k_1}{k_2}}\beta < \beta \leq r \tag{58}$$

if there exist $r > 0$ and a continuously differentiable function $V(t,x)$ satisfying the conditions

$$k_1||x||^2 \leq V(t,x) \leq k_2||x||^2, \tag{59}$$
$$k_3||x||^2 \leq -\dot{V}(t,x), \tag{60}$$

for all $x \in \overline{B(r)}$, $t \in \Gamma$. Here, $k_i > 0$, $i = 1, 2, 3$, $||x||$ is the Euclidean norm, and the time interval length T is such that

$$T > \frac{k_2}{k_3} \cdot \ln\frac{k_2}{k_1}. \tag{61}$$

Proof: Condition (60) implies that

$$\dot{V}(t,x) \leq 0, \quad \forall\ x\ \in\ \overline{B(\beta)}, \quad t\ \in\ \Gamma.$$

Hence, it is implied by Lemma 4 that (50) is uniformly finite-time stable with respect to $(\alpha, \beta, \Gamma, ||\cdot||)$ for any α, β satisfying condition (58). Next, we prove quasi-contractive stability of the system. From conditions (59) and (60), we have

$$\dot{V}(t,x) \leq -\frac{k_3}{k_2}V(t,x), \quad \forall\, x \in\ \overline{B(r)}, \quad t\ \in\ \Gamma.$$

Hence,

$$V(t,\phi(t;t_0,x_0)) \leq V(t_0,x_0)\exp(-\frac{k_3}{k_2}(t-t_0)), \quad \forall\, x_0 \in \overline{B(r)}, \quad t \in \Gamma.$$

Then it follows from (59) that

$$||\phi(t;t_0,x_0)||^2 \leq \frac{k_2}{k_1}||x_0||^2\exp(-\frac{k_3}{k_2}(t-t_0)), \quad \forall\, x_0 \in \overline{B(r)}, \quad t \in \Gamma.$$

Thus, there exists a $t_1 \in \Gamma$ so that $||\phi(t;t_0,x_0)|| < \gamma, \forall\, t \in [t_1, t_0+T)$ when conditions (58) and (61) hold. Then according to Definition 3, system (50) is quasi-contractively stable with respect to $(\alpha,\gamma,\Gamma,||\cdot||)$ for any α,γ satisfying (58).

□

VI.2. Application to Deployment

In the following discussion, we consider the deployment of the subsatellite of the tethered satellite system. For simplicity, let $\dot{\ell} > 0$ throughout deployment. By Eq. (41), we have

$$\dot{\ell} > 0 \iff -\frac{\Omega r_0}{2}(1-\frac{r_0^3}{(\hat{r}_m^*(\ell))^3})\sin\theta^* > 0$$

From the discussion above and Eq. (42), the condition on θ^* for $\dot{\ell} > 0$ is that either $\theta_2(\ell_f) < \theta^* < \pi$, or $-\frac{\pi}{2} < \theta^* < 0$ (see Figure 3), where $\theta_2(\ell_f)$ solves

$$\cos\theta_2 = -\frac{\ell_f}{2r_0}, \quad 0 < \theta_2 < \pi \tag{62}$$

and ℓ_f is the desired post-deployment tether length.

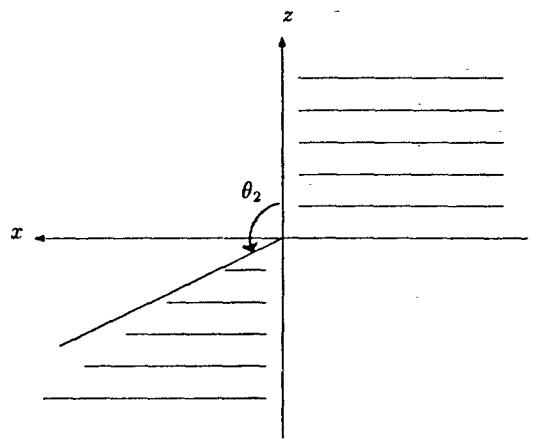

Figure 3. Deployment Regions for θ^* with $\phi^* = 0$

Two strategies for deployment are considered here. The first consists of the constant in-plane angle control law for deployment, and the second involves following the constant in-plane angle control law followed by a stabilizing station-keeping control once the desired in-plane angle is close enough to 0 radians or π radians.

Strategy 1. Constant Angle Control Only

We now consider application of the constant in-plane angle control law discussed above to subsatellite deployment. In the following, ℓ_f denotes the desired final tether length and ℓ_i denotes the initial tether length supported by a boom.

From (41), we have

$$\begin{aligned}\frac{\dot{\ell}}{\ell} &= -\frac{\Omega r_0 \sin\theta^*}{2\ell}\left(1 - \frac{r_0}{(\hat{r}_m^*(\ell))^3}\right) \\ &= -\frac{\Omega \sin\theta^*}{2} \cdot \frac{r_0}{\ell} \cdot \frac{(\hat{r}_m^*(\ell))^6 - r_0^6}{(\hat{r}_m^*(\ell))^3[r_0^3 + (\hat{r}_m^*(\ell))^3]} \\ &\geq -\Omega \sin\theta^* \cos\theta^* > 0 \end{aligned} \tag{63}$$

for any $\theta^* \in S_d$ and $\ell_i \leq \ell \leq \frac{1}{22} r_0$, where

$$S_d := \{\theta^* | -0.68 \text{ radians } \leq \theta^* < 0, \text{ or } 2.5 \text{ radians } \leq \theta^* < \pi \text{ radians}\}.$$

Hence, $\frac{\dot{\ell}}{\ell}$ is bounded below for all $\ell_i \leq \ell \leq \ell_f$ and $\theta^* \in S_d$, and similarly for $\dot{\ell}$. Thus, for any $\ell_f > \ell_i$, ℓ will increase past ℓ_f at some $T > 0$. Theorem 5 below asserts that the system will be finite-time contractively stable during deployment over the interval $[t_0, t_0+T)$, near the equilibrium point $(\theta^*, 0, 0, 0)$ with $\theta^* \in S_d$.

Theorem 5. Suppose $\Omega < 1$, $\ell_f \leq \frac{1}{22} r_0$, and $\Gamma := [t_0, t_0 + T)$. There is an $r > 0$ such that system (33)-(36) is finite-time contractively stable with respect to $(\alpha, \beta, \gamma, \Gamma, \|\cdot\|)$ at the equilibrium point $(\theta^*, 0, 0, 0)$ for any α, β, γ and T satisfying (58) and (61), if either of following two conditions on the desired in-plane angle θ^* holds:

(i) -0.68 radians $\leq \theta^* < 0$

(ii) 2.5 radians $\leq \theta^* < \pi$ radians

Proof: Let $m := \Omega \sin 2\theta^*$, then it is clear from (63) that

$$-\frac{2\dot{\ell}}{\ell} \leq m < 0, \quad \forall\ t \in \Gamma,$$

if either of conditions (i) and (ii) holds and $\frac{1}{22} r_0 \leq \ell_f \leq \ell$. Invoking the finite-time stability criteria given in Section VI.1, the stability of the TSS during constant angle deployment can be proved as follows.

Using a general construction [18] for a class of systems of the form (48)-(49), we prove the finte-time contractive stability of (33)-(36) during deployment by employing the Liapunov-like function

$$\begin{aligned} V(t, \tilde{\theta}, \omega_\theta, \phi, \omega_\phi) = (\frac{2\dot{\ell}}{\ell} + \frac{n_1(t)}{m})\tilde{\theta}^2 + 2\tilde{\theta}\omega_\theta - \frac{1}{m}\omega_\theta^2 \\ + (\frac{2\dot{\ell}}{\ell} + \frac{n_2(t)}{m})\phi^2 + 2\phi\omega_\phi - \frac{1}{m}\omega_\phi^2, \end{aligned} \tag{64}$$

where

$$n_1(t) := 2\Omega\frac{\dot{\ell}}{\ell}\cot\theta^* + \frac{3\Omega^2 r_0^5}{(\hat{r}_m^*(\ell))^5}\sin^2\theta^*, \tag{65}$$

$$n_2(t) := -\Omega^2 + 2\Omega\frac{\dot{\ell}}{\ell}\cot\theta^*. \tag{66}$$

Then corresponding to the original system (33)-(36), we have

$$\dot{V}(t,\tilde{\theta},\omega_\theta,\phi,\omega_\phi) = n_3(t)\tilde{\theta}^2 + n_4(t)\phi^2 + 2(1+\frac{2\dot{\ell}}{m\ell})\cdot(\omega_\theta^2+\omega_\phi^2)$$
$$+ 2(\tilde{\theta}-\frac{\omega_\theta}{m})f_1(t) + 2(\phi-\frac{\omega_\phi}{m})f_2(t), \tag{67}$$

where

$$f_1(t) = -\frac{2\dot{\ell}}{\ell}\Omega + 2\tan\phi(\omega_\theta+\Omega)\omega_\phi - \frac{\Omega^2 r_0\sin(\theta^*+\tilde{\theta})}{\ell\cos\phi}(1-\frac{r_0^3}{(\hat{r}_m^*(\ell))^3}) - n_1(t)\tilde{\theta}, \tag{68}$$

$$f_2(t) = -\frac{1}{2}\sin(2\phi)(\omega_\theta+\Omega)^2 - \frac{\Omega^2 r_0}{\ell}\cos(\theta^*+\tilde{\theta})\sin\phi(1-\frac{r_0^3}{(\hat{r}_m^*(\ell))^3}) - n_2(t)\phi, \tag{69}$$

and

$$n_3(t) = 2n_1(t) + \frac{d}{dt}\{\frac{2\dot{\ell}}{\ell}\} + \frac{1}{m}\cdot\frac{dn_1(t)}{dt}, \tag{70}$$

$$n_4(t) = 2n_2(t) + \frac{d}{dt}\{\frac{2\dot{\ell}}{\ell}\} + \frac{1}{m}\cdot\frac{dn_2(t)}{dt}. \tag{71}$$

First, consider the case in which θ^* satisfies condition (i). After some calculations using (64)-(66), we find that there exist $k_{1,1}$, $k_{1,2} > 0$ (given in the Appendix) such that

$$k_{1,1}||x||^2 \le V(t,\tilde{\theta},\omega_\theta,\phi,\omega_\phi) \le k_{1,2}||x||^2,\ \forall\ t\in\Gamma, \tag{72}$$

where $x = (\tilde{\theta},\omega_\theta,\phi,\omega_\phi)^T$ and the norm indicated is the Euclidean norm. Moreover, by choosing $k_{1,3} := 0.132\Omega^2$ and

$$r = \sup_{t\in\Gamma}\{\ ||x||\ :\ |f_1| \le \frac{mk_{1,3}||x||}{2(m-1)} \quad\text{and}\quad |f_2| \le \frac{mk_{1,3}||x||}{2(m-1)}\}, \tag{73}$$

we have

$$-\dot{V}(t,\tilde{\theta},\omega_\theta,\phi,\omega_\phi) \ge k_{1,3}||x||^2,\ \forall\ t\in\Gamma,\quad x\in\ \overline{B(r)}. \tag{74}$$

Thus, conditions (59)-(60) are satisfied and the conclusion follows from Theorem 4.

Similarly, for the case in which θ^* satisfies condition (ii), we have

$$k_{2,1}||x||^2 \le V(t,\tilde{\theta},\omega_\theta,\phi,\omega_\phi) \le k_{2,2}||x||^2,\ \forall\ t\in\Gamma, \tag{75}$$

where $k_{2,1}$, $k_{2,2} > 0$ are also specified in the Appendix. By choosing $k_{2,3} := 0.0442\Omega^2$ and

$$r = \sup_{t\in\Gamma}\{\ ||x||\ :\ |f_1| \le \frac{mk_{2,3}||x||}{2(m-1)} \quad \text{and} \quad |f_2| \le \frac{mk_{2,3}||x||}{2(m-1)}\}, \tag{76}$$

we guarantee that

$$-\dot{V}(t,\tilde{\theta},\omega_\theta,\phi,\omega_\phi) \ge k_{2,3}||x||^2,\ \forall\, t\in\Gamma,\quad x\in\ \overline{B(r)}. \tag{77}$$

The conclusion again follows from Theorem 4.

□

The finite-time contractive stable regions of the desired in-plane angle θ^* for constant in-plane angle deployment are given in Theorem 5. In addition, a relationship between the time-interval T, the bound of initial disturbances and the final contracted region is set up in Theorem 4. Furthermore, the simulation results given in Section VII.2 shows that the criteria given in Theorem 5 are not vacuous.

Strategy 2. Station-Keeping Control Included

A tension control law has been designed in Section III to regulate the tether length at the point where the out-of-plane angle $\phi = 0$ and the in-plane angle $\theta = 0$ or $(\theta = \pi)$. Provided by Theorem 5 and the control strategies given in Theorems 1 and 2 (which design tension control law with linear state feedbacks and nonlinear state feedbacks from the Hopf bifurcation theorem), a switching control law for deployment can be set up as follows:

Step 1. Apply the constant angle control law (41) for the first step subsatellite deployment, in which the desired in-plane angle θ^* satisfies the conditions of Theorem 5 and closes to 0 radians (or π radians).

Step 2. Apply the tension control law given in Theorem 1 (or Theorem 2) once the tether length is sufficiently near the desired length ℓ_f.

It is supported by Theorem 5 that the initial disturbance states of the TSS can be contracted. Especially, with the desired in-plane angle is sufficiently near 0 or π radians, the system states of the TSS are expected to be contracted within the domain of attraction of the station-keeping control mode, after first step constant angle deployment. Hence, the tether length should be regulated to the desired length after switching to the stabilization

control proposed in Section III and [13] when the difference of the tether length with respect to the desired value is small enough. Thus, the TSS is concluded to be asymptotically stable for deployment by using this switching control law. Simulation results of a typical system given in Section VII.2 illustrate this conclusion.

VII. Simulation Results

Many simulation examples for tethered satellite systems in the station-keeping mode have been presented in [13]. In this section, we present simulation results only for deployment and retrieval.

A typical TSS with following characteristics is considered :

- Orbital radius $r_0 = 6598$ km,
- Subsatellite mass $m = 170$ kg,
- Orbital angular velocity $\Omega = 0.0011781$ radian/second.

In the following discussions, $\tilde{\theta} = \theta - \theta^*$ denotes the differential of the in-plane angle, ℓ_f denotes the desired final tether length, $\tilde{\ell} = \ell - \ell_f$ denotes the differential of the tether length and F_ℓ denotes the applied tension control force.

VII.1. Retrieval

As discussed in Section V, the set of candidate in-plane angles for constant angle retrieval is given by

$$S_r := \{\theta | 0 < \theta < \frac{\pi}{2} \quad \text{or} \quad -\pi < \theta < \theta_1(\ell_i)\},$$

where $\theta_1(\ell_i)$ is defined in (43). Let the initial disturbances of the system be $\phi = 0.01$ radians, $\tilde{\theta} = -0.01$ radians, and $\omega_\theta = \omega_\phi = 0$. The initial tether length ℓ_i is assumed to be 10 km. It is observed from Figures 4 and 5 that the equilibrium point $(\theta^*, 0, 0, 0)$ is unstable during retrieval with the desired in-plane angle $\theta^* = -3.0$ radians and $\theta^* = -1.6$ radians, respectively. As mentioned in [13], in reality, since the tether is not really rigid, the applied tension control force can not be positive to rule out compression. However, Figure 5 (d) shows that a positive tension control force F_ℓ occurs in some time interval. Thus, if a constant angle control law is applied during retrieval, then not only will the system be unstable, but also tether compression may occur.

It is also found that whenever the desired in-plane angle $\theta^* \in S_1 := \{-2.1 \text{ radians} < \theta^* < \theta_1(\ell_i)\}$ for constant angle retrieval, the applied tension control force F_ℓ can have positive value in some time-interval, i.e., compression may occur. The system response of $\theta^* = -2.1$ radians for constant retrieval is depicted in Figure 6, where F_ℓ is found (see Figure 6 (d)) to be very close to 0 at some time instant but never greater than 0.

Similar simulation results are found for the region $0 < \theta^* < \frac{\pi}{2}$ for constant angle retrieval. The equilibrium point $(\theta^*, 0, 0, 0)$ is found unstable during retrieval and the compression of the tether may occur in case $1.0 < \theta^* < \frac{\pi}{2}$. The system responses are not shown.

VII.2. Deployment

According to Theorem 5, the set of candidate θ^* for stable deployment is

$$S_d = \{\theta | -0.68 \text{ radians } \leq \theta < 0, \quad \text{or} \quad 2.5 \text{ radians } \leq \theta < \pi \text{ radians}\}.$$

Let the initial disturbances of the system be $\phi = 0.01$ radians, $\tilde{\theta} = -0.01$ radians, and $\omega_\theta = \omega_\phi = 0$. The initial tether length is assumed to be $\ell_i = 10$ m, which is provided by a boom. First, the system response during deployment (applying constant in-plane angle control only) are depicted in Figures 7 and 8, with $\theta^* = -0.68$ radians, and $\theta^* = 2.5$ radians, respectively. It is observed from the system responses that, for example, the differential of the in-plane angle $\tilde{\theta}$ and the out-of-plane angle ϕ, decay during deployment.

The switching control strategy, which involves both constant angle control and station-keeping control, is applied to deploy a subsatellite from the satellite with the desired final tether length $\ell_f = 10$ km. The first example considers to deploy the subsatellite upward (i.e., away from the Earth) by applying constant angle control with $\theta^* = -0.015$ for first 260,500 seconds, and applying the station-keeping control thereafter. The applied tension control force for station-keeping is governed by

$$F_\ell = -m(U + h_1\tilde{\ell} + h_2\dot{\ell}), \tag{78}$$

where $U = 0.041019$, $h_1 = 3.1\Omega^2$ and $h_2 = 0.0034$. The responses of the system during constant angle deployment are shown in Figure 9. At time $t = 260,500$ seconds, we have

- the out-of-plane angle $\phi = -7.01636 \times 10^{-6}$ radians and

$\dot{\phi} = 1.70633 \times 10^{-8}$ radian/second

- the in-plane angle $\theta = -0.0150051$ radians and $\dot{\theta} = 5.61812 \times 10^{-10}$ radian/second
- the actual tether length $\ell = 9.97617$ km and $\dot{\ell} = 2.63603 \times 10^{-4}$ km/second.

With these values, the applied tension control law is switched to the station-keeping control and governed by Eq. (78). The system responses governed by (78) are depicted in Figure 10.

Another example for deploying subsatellite downward (i.e., toward the Earth) is implemented by applying constant angle control for the first 235,300 seconds with $\theta^* = 3.125$ radians, then switched to the station-keeping control governed by Eq. (78). At time $t = 235,300$ seconds, we have

- the out-of-plane angle $\phi = -2.01378 \times 10^{-6}$ radians and
  $\dot{\phi} = -2.35517 \times 10^{-8}$ radian/second
- the in-plane angle $\theta = 3.1250$ radians and $\dot{\theta} = 8.96566 \times 10^{-9}$ radian/second
- the actual tether length $\ell = 9.88531$ km and $\dot{\ell} = 2.90670 \times 10^{-4}$ km/second.

The system responses are shown in Figures 11 and 12.

Acknowledgment

The authors thank Professors P.S. Krishnaprasad and J.H. Maddocks for helpful discussions. This research was supported in part by the Air Force Office of Scientific Research under URI Grant AFOSR-87-0073, and by the NSF under Grants ECS-86-57561 and CDR-85-00108.

References

[1] C. C. Rupp and J. H. Laue, "Shuttle/tethered satellite system," *The Journal of the Astronautical Sciences*, Vol. 26, pp. 1-17, 1978.

[2] D. A. Arnold, "The behavior of long tethers in space," *The Journal of the Astronautical Sciences*, Vol. 35, pp. 3-18, 1987.

[3] J. B. Eades, Jr. and H. Wolf, *Tethered Body Problems and Relative Motion Orbit Determination*, Final Report, Contract NAS5-21453, Analytical Mechanics Associates, Inc., Seabrook, MD, 1972.

[4] T. R. Kane and A. K. Banerjee, "Tether deployment dynamics," *The Journal of*

the Astronautical Sciences, Vol. 30, pp. 347-365, 1982.

[5] C. C. Rupp, *A Tether Tension Control Law for Tethered Subsatellites Deployed Along Local Vertical*, NASA TM X-64963, 1975.

[6] A. K. Misra and V. J. Modi, "Deployment and retrieval of shuttle supported tethered satellites," *J. Guidance*, Vol. 5, pp. 278-285, 1980.

[7] P. M. Bainum, S. Woodard and J. Juang, "The development of optimal control laws for orbiting tethered platform systems," AAS 85-360, pp. 41-55, 1985.

[8] W. P. Baker, J. A. Dunkin, Z. J. Galaboff, K. D. Johnston, R. R. Kissel, M. H. Rheinfurth and P. L. Siebel, *Tethered Subsatellite Study*, NASA TM X-73314, 1976.

[9] E. H. Abed and D.-C. Liaw, "On the stabilization of tethered satellite systems," *Abstracts of the Second Conf. on Non-Linear Vibrations, Stability, and Dynamics of Structures and Mechanisms*, VPI, Blacksburg, VA, June 1988.

[10] R. W. Brockett, *Finite Dimensional Linear Systems*, John Wiley and Sons, Inc. 1969.

[11] D.-C. Liaw and E. H. Abed, "Stability analysis and control of tethered satellites," *Model Determination for Large Space Systems Workshop*, Rept. JPL D-5574, Jet Propulsion Laboratory, Pasadena, CA, pp. 308-330, 1988.

[12] NASA, Mission Planning and Analysis Division, *Space Station Mission Requirements Data Base*, Rept. JSC-32072, NASA Space Station Program Office, Reston, VA, May 1988.

[13] D.-C. Liaw and E. H. Abed, "Nonlinear stabilization of tethered satellites," in *Proc. 27th IEEE Conf. Decision and Control*, Austin, TX, pp. 1738-1745, 1988.

[14] J. L. Kaplan, "Converse theorems for finite-time stability and practical stability," *IEEE Trans. Circuit Theory*, Vol. CT-20, pp. 66-67, 1973.

[15] E. H. Abed and J.-H. Fu, "Local feedback stabilization and bifurcation control, I. Hopf bifurcation," *Systems and Control Letters*, Vol. 7, pp. 11-17, 1986.

[16] D.-C. Liaw and E. H. Abed, *Stabilization of Tethered Satellites During Station-Keeping*, Rept. TR 88-72, Systems Research Center, Univ. of Maryland, College Park, 1988. Submitted for publication.

[17] W. Hahn, *Stability of Motion*, Springer-Verlag, New York Inc. 1967.

[18] D.-C. Liaw and E. H. Abed, "Possible bounds on finite-time stability," in preparation.

Appendix

The values of $k_{i,j}$, $i = 1, 2$ and $j = 1, 2$ are as given below.

$$k_{1,1} = \frac{0.295575407 \csc^2 2\theta^*}{k_{1,2}},$$

$$k_{1,2} = \frac{l_1 + l_2 + \sqrt{(l_1 + l_3)^2 + 4}}{2},$$

$$k_{2,1} = \frac{0.498328311 \csc^2 2\theta^*}{k_{2,2}},$$

$$k_{2,2} = \frac{l_4 + l_5 + \sqrt{(l_4 + l_6)^2 + 4}}{2},$$

where

$$l_1 = -3\Omega \cos\theta^* \sin\theta^* - 0.5\Omega \sin\theta^*,$$

$$l_2 = -\frac{\Omega^2(3\cos^2\theta^* + 0.5\cos\theta^*) + 1}{\Omega \sin 2\theta^*},$$

$$l_3 = -\frac{\Omega^2(3\cos^2\theta^* + 0.5\cos\theta^*) - 1}{\Omega \sin 2\theta^*},$$

$$l_4 = -3.68961\Omega \cos\theta^* \sin\theta^*,$$

$$l_5 = -\frac{3.6896061\Omega^2 \cos^2\theta^* + 1}{\Omega \sin 2\theta^*},$$

$$l_6 = -\frac{3.6896061\Omega^2 \cos^2\theta^* - 1}{\Omega \sin 2\theta^*}.$$

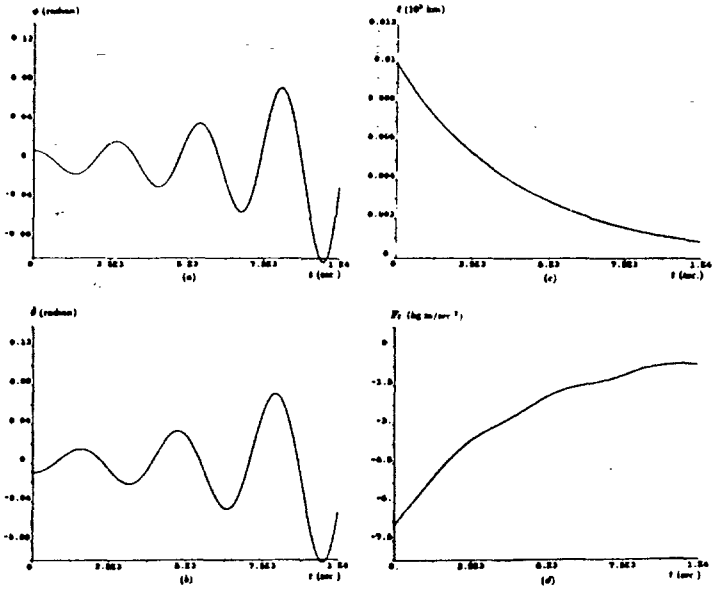

Figure 4. Simulation Results for Constant Angle Retrieval with $\theta^* = -3.0$ radians

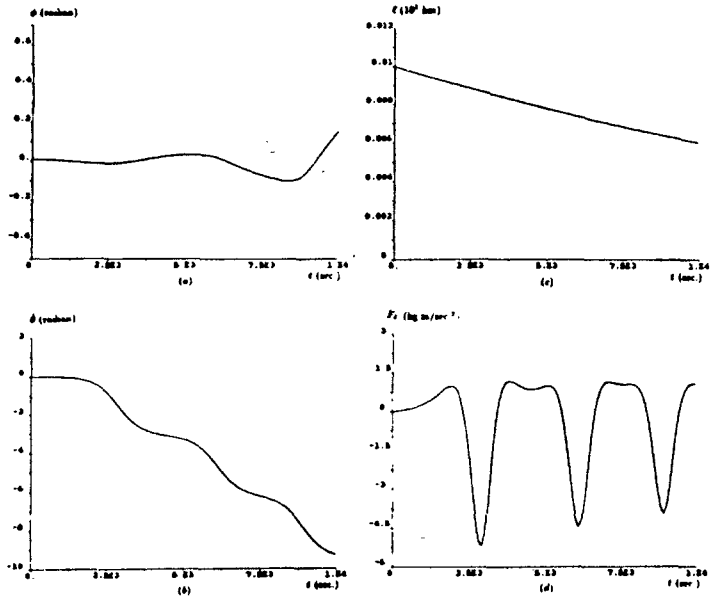

Figure 5. Simulation Results for Constant Angle Retrieval with $\theta^* = -1.6$ radians

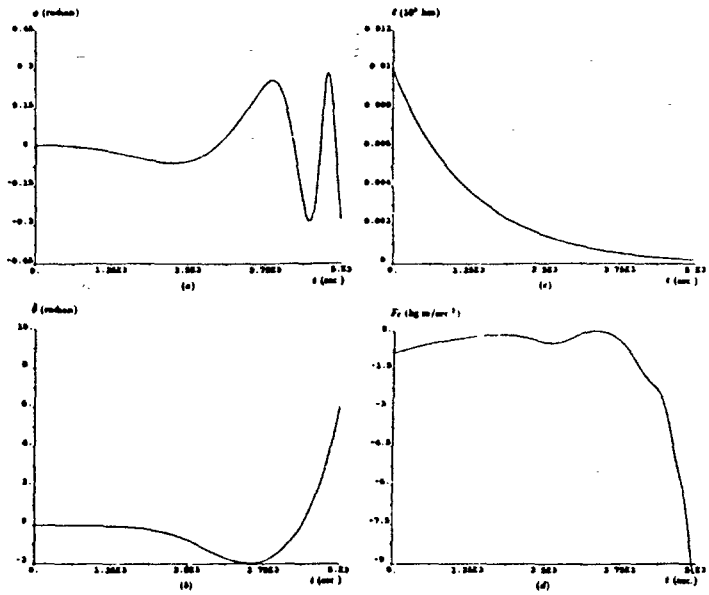

Figure 6. Simulation Results for Constant Angle Retrieval with $\theta^* = -2.1$ radians

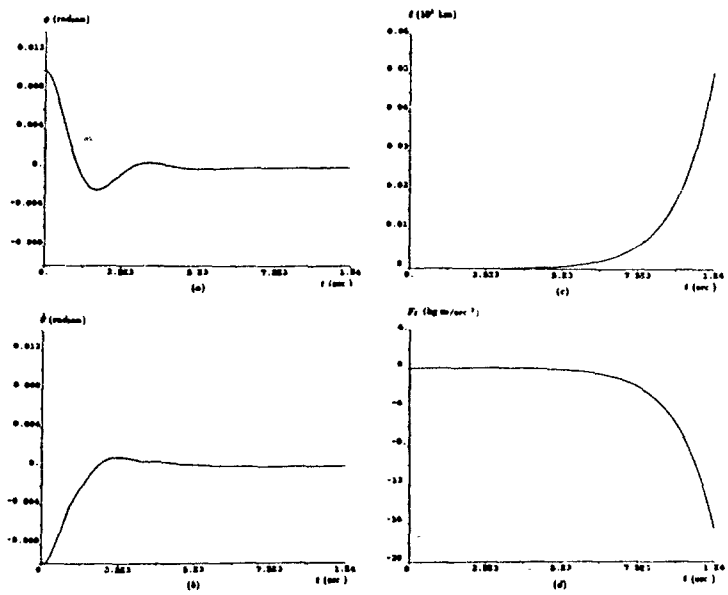

Figure 7. Simulation Results for Constant Angle Deployment with $\theta^* = -0.68$ radians

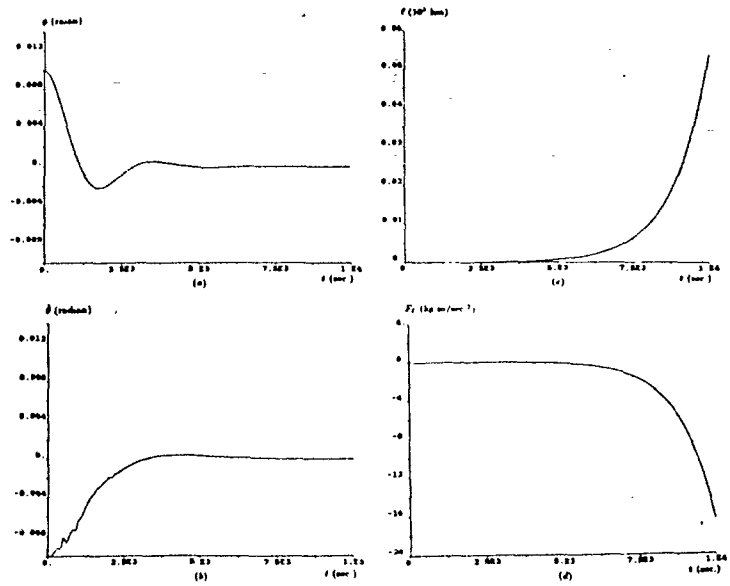

Figure 8. Simulation Results for Constant Angle Deployment with $\theta^* = 2.5$ radians

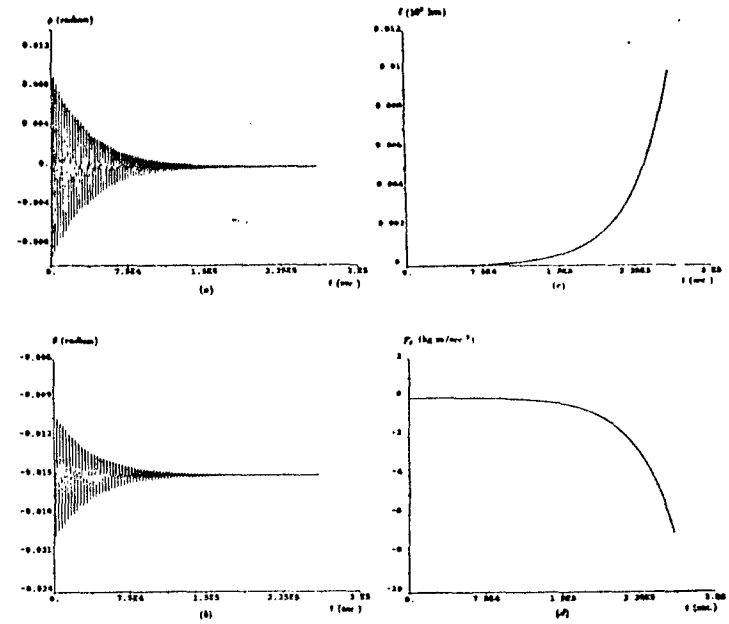

Figure 9. Simulation Results for Constant Angle Deployment with $\theta^* = -0.015$ radians

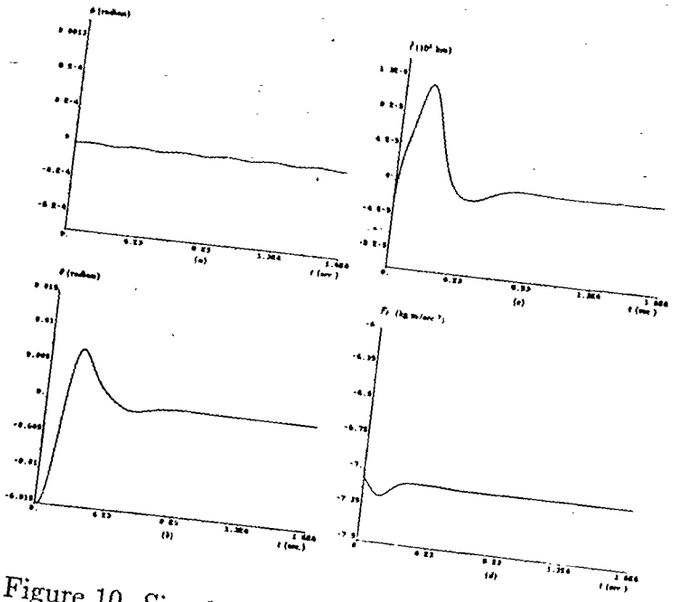

Figure 10. Simulation Results for Station-Keeping

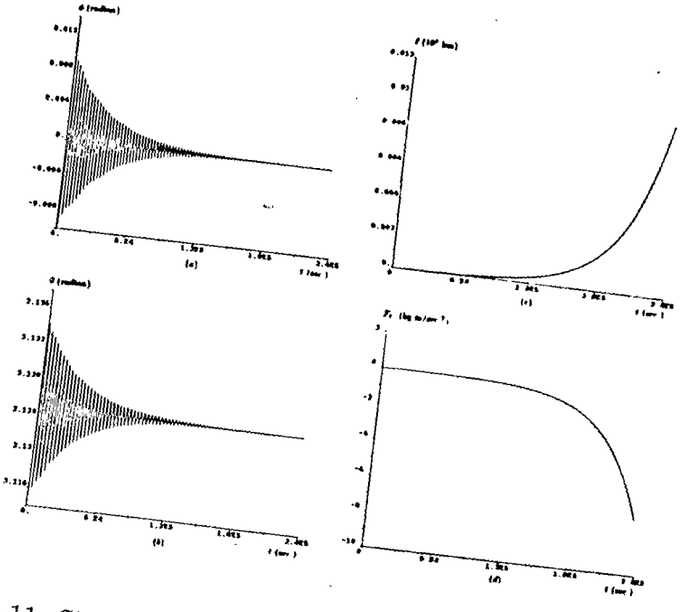

Figure 11. Simulation Results for Constant Angle Deployment with $\theta^* = 3.125$ radians

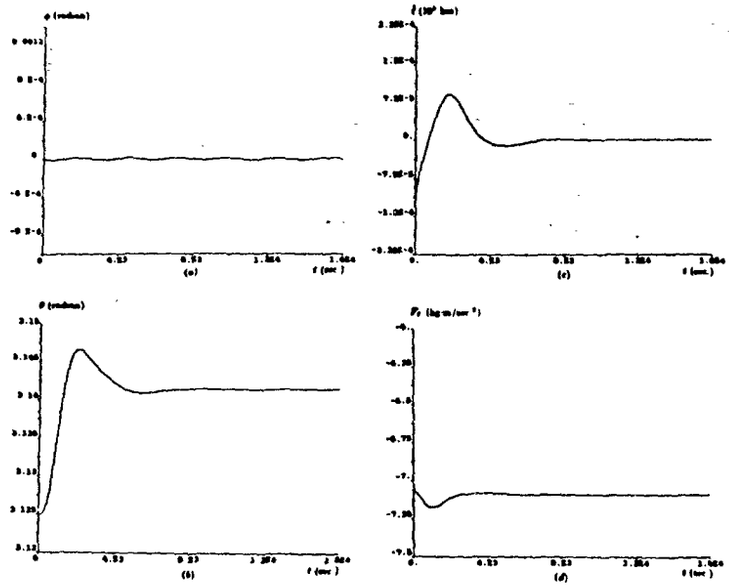

Figure 12. Simulation Results for Station-Keeping with $\theta^* = \pi$ radians